Clay Minerals, (2007) **42**, 187–201

Clay mineral genesis and chemical evolution in the Miocene sediments of Somosaguas, Madrid Basin, Spain

O. FESHARAKI[1], E. GARCÍA-ROMERO[1,*], J. CUEVAS-GONZÁLEZ[2] AND N. LÓPEZ-MARTÍNEZ[3]

[1] *Departamento de Cristalografía y Mineralogía, Facultad de Ciencias Geológicas, Universidad Complutense de Madrid, Spain,* [2] *Departamento Ciencias de la Tierra y del Medio Ambiente, Universidad de Alicante, Spain, and* [3] *Departamento de Paleontología, Facultad de Ciencias Geológicas, Universidad Complutense de Madrid, Spain*

(*Received 27July 2006; revised 7 February 2007*)

ABSTRACT: A mineralogical and microtextural study of Somosaguas Miocene deposits, located in the Madrid Basin (western Madrid, Spain), was carried out using X-ray diffraction, scanning electron microscopy, transmission electron microscopy and optical microscopy, whereas crystal chemistry data were obtained by analytical electron microscopy-transmission electron microscopy and electron icroprobe analysis. Four stratigraphic sections were studied, compising detrital rocks representing intermediate and distal facies from alluvial fan deposits. The predominant source area of these sediments was the granitic rocks of the Spanish Central System with a lesser contribution of metamorphic rocks. Clayey arkoses are the most abundant rocks of these sections, typical of granite alteration under warm, semi-arid climates. The mineralogy is characterized by phyllosilicates, followed by feldspars and quartz. The data obtained reveal mineral mixtures of detrital (quartz, feldspars, kaolinite, micas and chlorite), transformed (illite and beidellite) and neoformed (montmorillonite) origin. Clay minerals resulted from interactions between detrital minerals and meteoric waters. Two trends of degradation of micas are detected. The first shows a transition from muscovites and dioctahedral illites, to beidellites. The other trend is defined by the biotite degradation to beidellites with different layer charge and octahedral Fe content. Montmorillonites were neoformed from the hydrolysis and weathering of primary minerals (feldspars and muscovite). Magnesian clay minerals such as sepiolite, palygorskite and trioctahedral smectites, extremely abundant in the centre of the basin, were not detected in Somosaguas sediments.

KEYWORDS: Madrid basin, Somosaguas, Miocene, arkoses, altered biotite, beidellite, montmorillonite.

The Tajo Basin is one of the intracratonic Cenozoic basins of the Iberian Península formed in relation to the convergence between the African and European plates (Vegas & Banda, 1982; De Vicente *et al*., 1996a), the proto-Atlantic ocean formation and the structuring of the Western Mediterranean Basin. All these processes fit in the Alpine Orogeny dynamics. The Tajo Basin has an approximately triangular morphology, bordered by three mountain ranges with different lithologies and origins: the Central System at the north and west, the Iberian Range at the east and the Toledo Mountains at the south. During the Upper Paleogene it was subdivided into two smaller basins by the North-South uplift of Altomira Range (Alonso-Zarza *et al*., 2004), leaving the Madrid Basin at the west and the smaller Loranca Basin at the east. The basement of the Madrid Basin broke during the Alpine Orogeny (De Vicente *et al*., 1996a), and was subsequently filled mainly with tertiary sediments, predominantly of Paleogene age in depth and Neogene age at the surface (Alonso-Zarza *et al*., 2004).

* E-mail: mromero@geo.ucm.es
DOI: 10.1180/claymin.2007.042.2.05

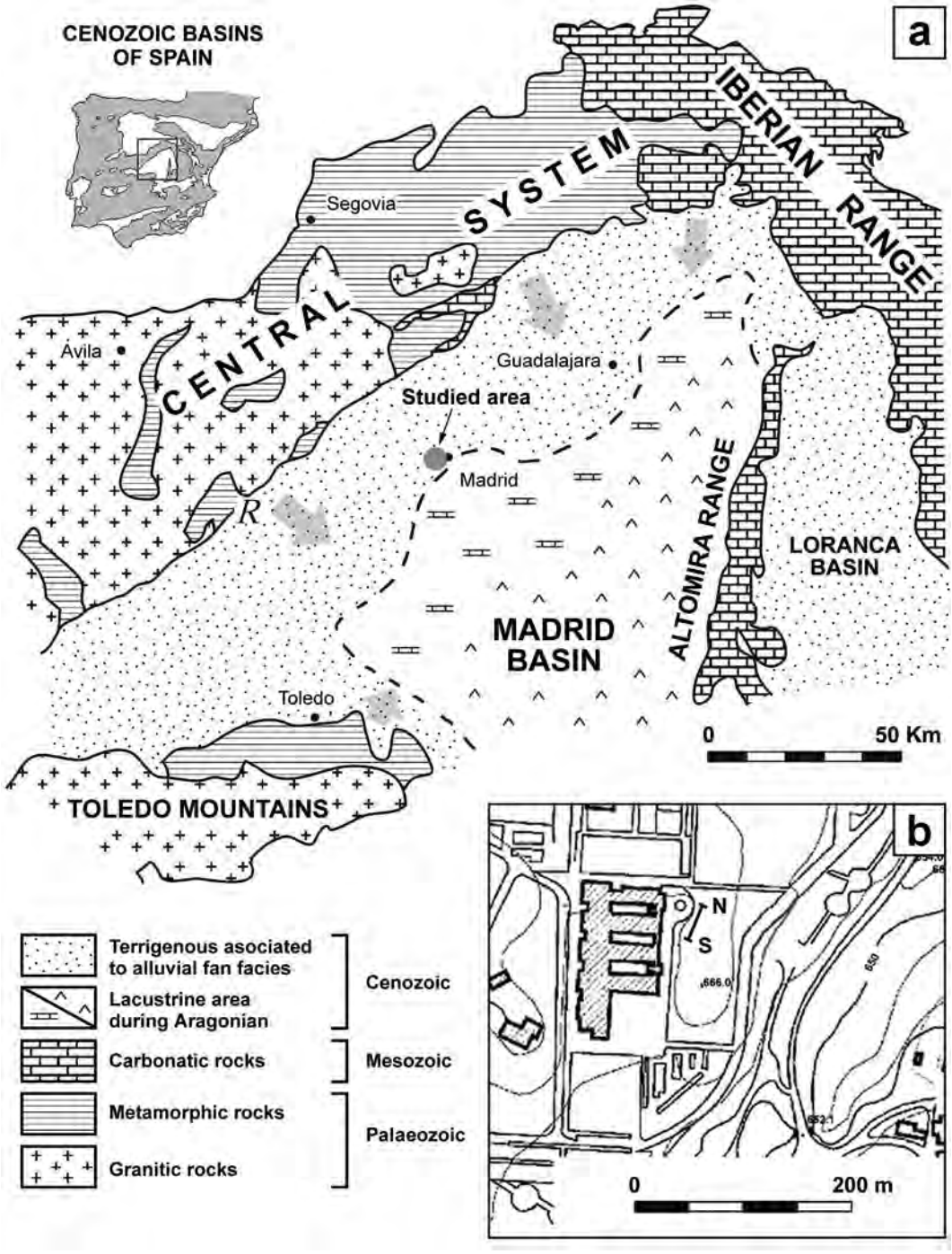

FIG. 1. Location maps of the studied sediments. (a) Geological map showing the distribution of facies of the Intermediate Unit of the Madrid Basin Miocene sediments (modified from Calvo *et al*. 1989). (b) Detail of the studied area (Somosaguas).

From a sedimentological point of view, the most remarkable characteristic of the Neogene Madrid deposits is their great variety of facies and the complexity of lateral changes, due to very active detrital sedimentation of materials from the erosion of the surrounding mountain systems. The studied deposits in the Somosaguas zone (western Madrid Basin), dated as Middle Miocene (Aragonian ≈ 14 m.y.; Luis & Hernando, 2000), belong to the Intermediate Unit (Megías *et al*., 1982). From bottom to top, the Intermediate Unit contains detrital gypsum beds lying above karstic surfaces on the underlying gypsum deposits (Lower Unit). Above it, a change from sulphate to carbonate sedimentation is recorded, followed finally by significant progradation of detrital materials from the northern and western borders toward the centre of the basin (Ordóñez *et al*., 1983; Calvo *et al*., 1984). These progradational alluvial fan systems consist of several facies belts (Alonso-Zarza *et al*., 2004). In their proximal zones, they consist of conglomerates and coarse-grained arkosic sandstones; in middle zones, finer-grained arkosic sandstones intercalated with lutites; in distal zones the clayey levels dominate, with intercalations of micaceous sands, gypsum and carbonates (Lomoschitz *et al*., 1985). Micaceous sands have been related to transitional facies between the proximal and central areas, where levels of carbonates were deposited in marsh or shallow lake environments (Bustillo, 1976; Bustillo & Bustillo, 1988; Bustillo & Capitán, 1990). The most central facies of the Intermediate Unit contain mainly detrital gypsum. These deposits contain Mg-rich clays which are of great economic interest (Regueiro *et al*., 2002).

The main factors that affected the genesis of the Middle Miocene materials studied are: (1) a source area mainly consisting of granitoids and gneiss (Villaseca *et al*., 1993), (2) an active compressional tectonic regime (De Vicente *et al*., 1996a,b), and (3) a hot palaeoclimate with well marked seasons (López-Martínez *et al*., 2000b).

The Somosaguas area, ~50 km from the NW border of the Madrid basin, contains very interesting palaeontological deposits discovered in 1989 and included in the Madrid Palaeontological Catalog (carta paleontológica de Madrid). They are the first Miocene deposits containing vertebrates from the western area of the basin (López-Martínez *et al*., 2000a; Polonio & López-Martínez, 2000). Up to now, two deposits containing vertebrate fossils have been discovered: Somosaguas North, rich in macrovertebrates, and Somosaguas South, rich in microvertebrates. These deposits are separated by a non-fossiliferous deposit (López-Martínez *et al*., 2000a; Polonio & López-Martínez, 2000).

The petrology and bulk mineralogy of the detrital facies of the Intermediate Unit have been well characterized at the northern, north-eastern and eastern part of the Madrid basin (Alonso-Zarza *et al*., 1990, 1992; Alonso-Zarza & Fort, 1991; Rodríguez Aranda *et al*., 1991, among others). Detailed mineralogical studies of detrital facies from the western central zone of the Basin were carried out by Dominguez-Diaz (1994) and Dominguez-Diaz *et al*. (1996). The detrital materials of the western area have not yet been studied in detail. This is the major objective of the present study, which also covers the detailed mineralogical aspects of the Somosaguas deposits. The mineralogical study of the clay minerals from these sediments will aid understanding of the sedimentary processes during deposition of the Somosaguas deposits, as well as of the existence of genetic relations between the different mineral phases.

MATERIALS AND METHODS

The area studied is located in Pozuelo de Alarcón, near the western margin of the Madrid City, in the Somosaguas Campus of the Complutense University of Madrid (Fig. 1a,b). In this area, the most occidental vertebrate fossil site of the Madrid region appears at the western edge of the Tajo Basin, in arkosic sediments (Riba, 1959; Benayas *et al*., 1960).

Four stratigraphic sections have been studied (Fig 2). Different stratigraphic levels have been distinguished based on lithological diversity, structural and textural features of the sediments, and lateral continuity of the strata. Some levels have been described as lens-shaped bodies with little lateral continuity. Sixty samples representative of the four stratigraphic sections were collected. After grinding, chemical cementing agents were removed and separation of clay fractions was performed using methods suggested by Jackson (1975) and Moore & Reynolds (1989). The organic matter was oxidized by treating the carbonate-free samples with 30% H_2O_2, and digestion in a water bath. The cementing gypsum was eliminated by successive washings with hot water.

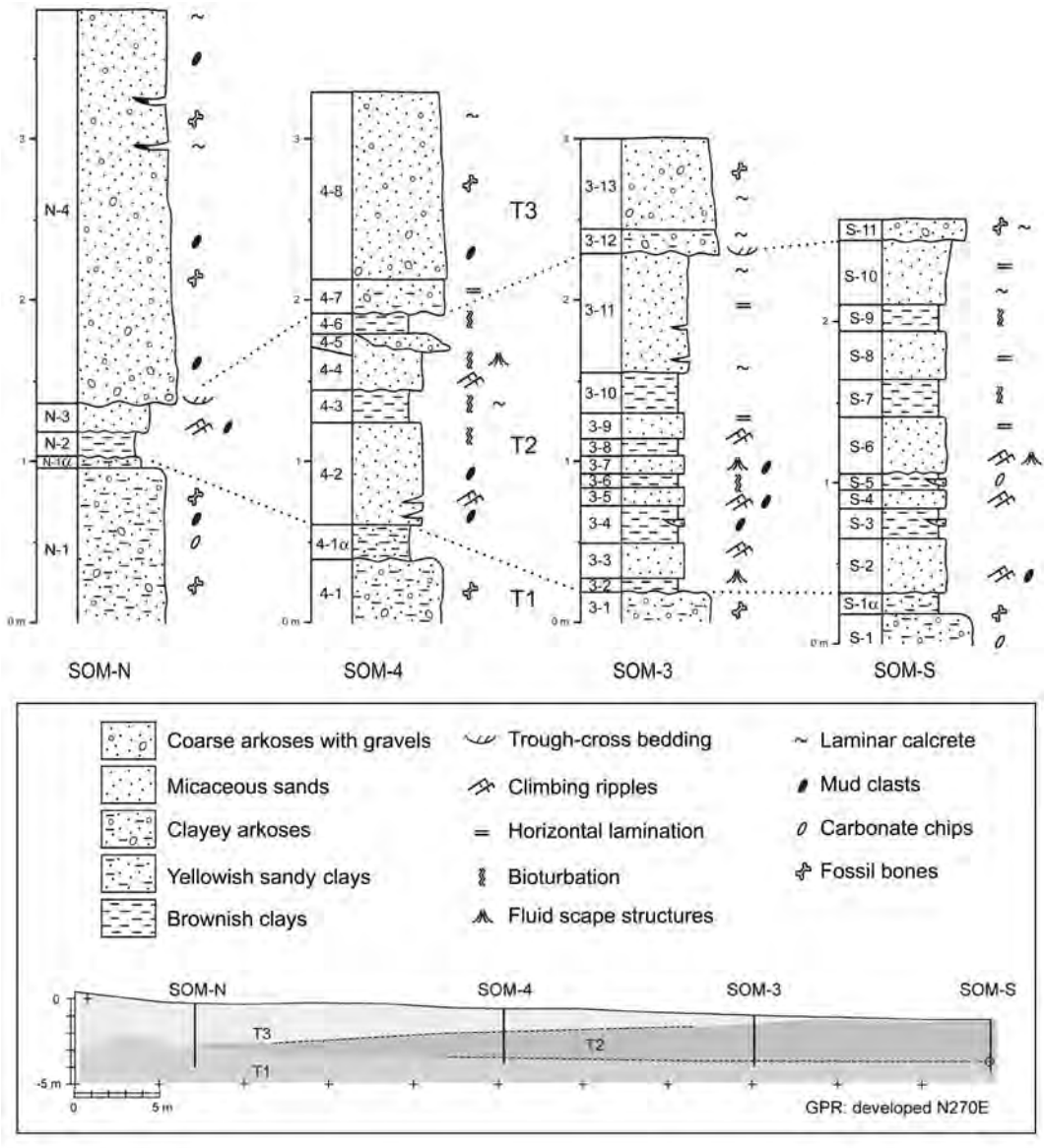

FIG. 2. Stratigraphic sections of the Somosaguas sediments showing the three different intervals distinguished. The numbers at the left of the sections indicate the sample name. The dashed lines indicate the correlation of the intervals between the four sections.

Mineralogical characterization was performed by X-ray diffraction (XRD) using a Siemens D500 diffractometer with Cu-$K\alpha$ radiation and a graphite monochromator. Bulk mineralogy was studied using random-powder specimens. Clay minerals were studied in the fractions <20 μm, <2 μm and <0.5 μm. The <2 μm clay fraction was obtained by sedimentation from an aqueous suspension according to Stokes' Law, and the <0.5 μm fraction by centrifugation. Oriented aggregates of air-dried clay, treated with ethylene glycol and heated at 550ºC/2 h, were studied. Random powders were scanned from 2−65º and oriented aggregates from 2−30º2θ, at a 0.02º2θ/s scan speed. Semiquantitative

determination of clay minerals was made according to Schultz's (1964) method. Optical microscopy was performed for petrographic study of detrital grains (feldspars and rock fragments) and textural relations among them.

Particle morphology and textural relationships were studied by scanning electron microscopy (SEM) and transmission electron microscopy (TEM). Scanning electron microscopy was performed on gold-coated broken surfaces of representative samples, using a JEOL, JSM 6400 microscope, operating at 40 kV and equipped with a Link System energy dispersive X-ray micro-analyser (EDX). Transmission electron microscopy was performed by depositing a drop of diluted suspension on microscopic copper grids covered by a collodion film.

The chemical composition of the clay minerals was obtained by analytical electron microscopy (AEM) with TEM, using a JEOL 2000 FX TEM microscope equipped with a double-tilt sample holder (up to a maximum of ±45º) at an acceleration voltage of 200 kV, with 0.5 mm zeta-axis displacement and 0.31 nm point-to-point resolution. The microscope incorporated an OXFORD ISIS energy dispersive X-ray spectrometer (136 eV resolution at 5.39 keV).

Electron microprobe analyses (EMPA) of detrital micas (predominantly biotites) were performed with wavelengh dispersive electron microprobe analysis (WDS-EPMA) on a JEOL JXA-8900M. Operating conditions included an accelerating voltage of 15 kV, a beam current of 20 nA and a beam diameter of 2−5 μm. The standards used are described by Jarosewich *et al*. (1980). Micaceous particles were hand picked from various sandy levels of the deposit, and they were embedded in a resin, cut in thin sections and coated with carbon. Several analyses have been carried out in the larger mica crystals to detect possible compositional variations.

Structural formulae of smectites and micas were calculated on the basis of 22 oxygen atoms per unit cell. Iron was considered as Fe^{2+} in the structural formulae of micas and Fe^{3+} in smectites. However, both can be present in the micas and smectites studied. We have considered Fe^{2+} in micas because usually Fe^{2+} is predominant in igneous or metamorphic rocks, but it should be taken into account that micas have undergone weathering processes and the Fe^{2+} oxidizes partially to Fe^{3+}. Unlike micas, smectites here usually have a greater proportion of Fe^{3+} than Fe^{2+}.

RESULTS

The mineralogical and chemical study permitted characterization of three intervals distinguished in the four stratigraphic sections (López-Martínez *et al*., 2000a; Mínguez Gandú, 2000; Fig. 2):

(1) The lower interval (T1) attributed to mud-flow currents, consists of clayey arkoses topped by a thin yellowish sandy clay level rich in micro-vertebrate fossils;

(2) The intermediate, barren lacustrine interval (T2), made up of intercalated layers of rippled micaceous sands and brownish clays; occasionally also channel-type arkosic lenses were found near the top. This interval wedges out and disappears towards the north of the area; and

(3) The upper interval (T3) of debris-flow deposits, consists of coarse-grained arkoses with large fossil bones. This interval fills an erosional hiatus which affected T2.

Mineralogy

The three stratigraphic intervals consist mainly of phyllosilicates (>50% of the total sample in all cases), feldspars (anorthite-rich plagioclase, orthoclase and microcline) (15−40%) and quartz (5−20%) (Table 1). Some levels also contain calcite, rutile, tourmaline and apatite. Gypsum is only present in the T1 interval. Rock fragments only appear in the T3 interval, and are generally made up of fine-grained plutonic and metamorphic rocks (mainly granites, gneiss, slates and quartzites). The main phyllosilicates are smectites (in some samples they constitute up to 90% of the clay fraction) and coarse micas (biotite and muscovite). Minor amounts of kaolinite are also present, as well as small amounts of mixed-layer illite-smectite (I-S), and highly altered chlorite. Mineralogy is relatively constant both between and within the different levels, although it changes in the different size fractions since smectites usually concentrate in the finer ones. Smectite abundance decreases and illite and kaolinite abundance increases with increasing particle size.

Mineral texture and morphology

In all lithologies, smectite forms typical honeycomb, cornflake and rose-like textures (Fig. 3a,b). The aggregates predominate in all lithologies, while the isolated flakes are predominant in the

TABLE 1. Mineralogical composition (%) of bulk samples and of the <20 μm, <2 μm and <0.5 μm fractions from XRD. The values have been rounded to 5 or 0 terminations, reflecting error bars. s = contents smaller than 3%. (Q = quartz; F = feldspars (potassium feldspar + plagioclase); Sm = smectites; I = illite; K = kaolinite).

						<0.5 μm			<2 μm			<20 μm	
Intervals	Samples	Lithology	Q	F	Sm	I	K	Sm	I	K	Sm	I	K
T3	N-4	Arkoses ss	10	25	60	s	5	50	5	10	50	10	5
	4-8		15	20	60	s	5	50	5	10	50	10	5
	3-13		15	20	55	5	5	50	5	10	50	10	5
	S-11		10	25	60	s	5	50	5	10	50	10	5
	4-7	Transitional arkoses	10	25	55	5	5	5	5	5	50	10	5
	3-12		10	30	50	5	5	50	5	5	50	10	10
	4-5	Canal	10	25	59	3	3	55	5	5	50	10	5
T2	N-2	Brownish clays	5	15	75	s	5	65	5	10	60	10	10
	4-6		5	15	70	5	5	65	5	10	65	5	10
	4-3		5	15	70	5	5	65	5	10	60	10	10
	3-10		5	15	70	5	5	65	5	10	60	10	10
	3-8		5	15	70	5	5	65	5	10	60	10	10
	3-6		5	15	70	5	5	60	10	10	60	10	10
	3-4		5	15	70	5	5	60	10	10	60	10	10
	3-2		5	15	70	s	10	65	5	10	60	10	10
	S-9		5	15	70	s	10	65	5	10	60	10	10
	S-7		5	15	70	5	5	65	5	10	60	10	10
	S-5		5	15	65	5	10	60	10	10	60	10	10
	S-3		5	15	70	5	5	65	5	10	60	10	10
	N-3	Micaceous sands	10	30	55	5	s	50	5	5	50	10	s
	4-4		10	30	55	s	5	55	5	s	50	5	5
	4-2		10	25	60	5	s	55	5	5	50	10	5
	3-11		10	40	45	s	5	45	5	s	40	5	5
	3-9		10	35	50	5	s	45	5	5	45	5	5
	3-7		10	35	50	5	s	45	5	5	40	10	5
	3-5		10	30	55	5	s	50	5	5	45	10	5
	3-3		10	30	55	5	s	50	5	5	45	10	5
	S-10		10	35	55	s	s	45	5	5	45	5	5
	S-8		10	35	50	5	s	45	5	5	45	5	5
	S-6		10	35	50	5	s	45	5	5	40	10	5
	S-4		10	30	55	5	s	50	5	5	45	10	5
	S-2		10	30	55	5	s	50	5	5	45	10	5
T1	N-1a	Yellowish clays	10	15	60	5	10	55	10	10	55	10	10
	4-1a		10	15	60	5	10	55	10	10	55	15	5
	S-1a		10	20	60	5	5	55	5	5	55	10	5
	N-1	Clayey arkoses	20	10	60	5	5	55	10	5	55	10	5
	4-1		15	15	60	5	5	50	10	10	50	15	5
	3-1		15	15	60	5	5	50	10	10	50	15	5
	S-1		15	15	60	5	5	50	10	5	50	15	5

brownish clay layers from T2. Sheets of open micas are frequent (Fig. 3c) with smectites growing on their edges and along fractures (Fig 3d). Most feldspars are partially dissolved, with smectite crystals growing on them, usually in the form of coatings (Fig. 3e,f). The TEM images allow the differentiation of two types of smectite particles. The first has very thin curved layers with warped edges and displays montmorillonite composition (Table 3, Fig. 4a), whereas the other type is idiomorphic forming flat crystallites (Beidellite composition, Fig. 4b). In many samples the beidellite particles display rounded-edge morphologies (Fig. 4c).

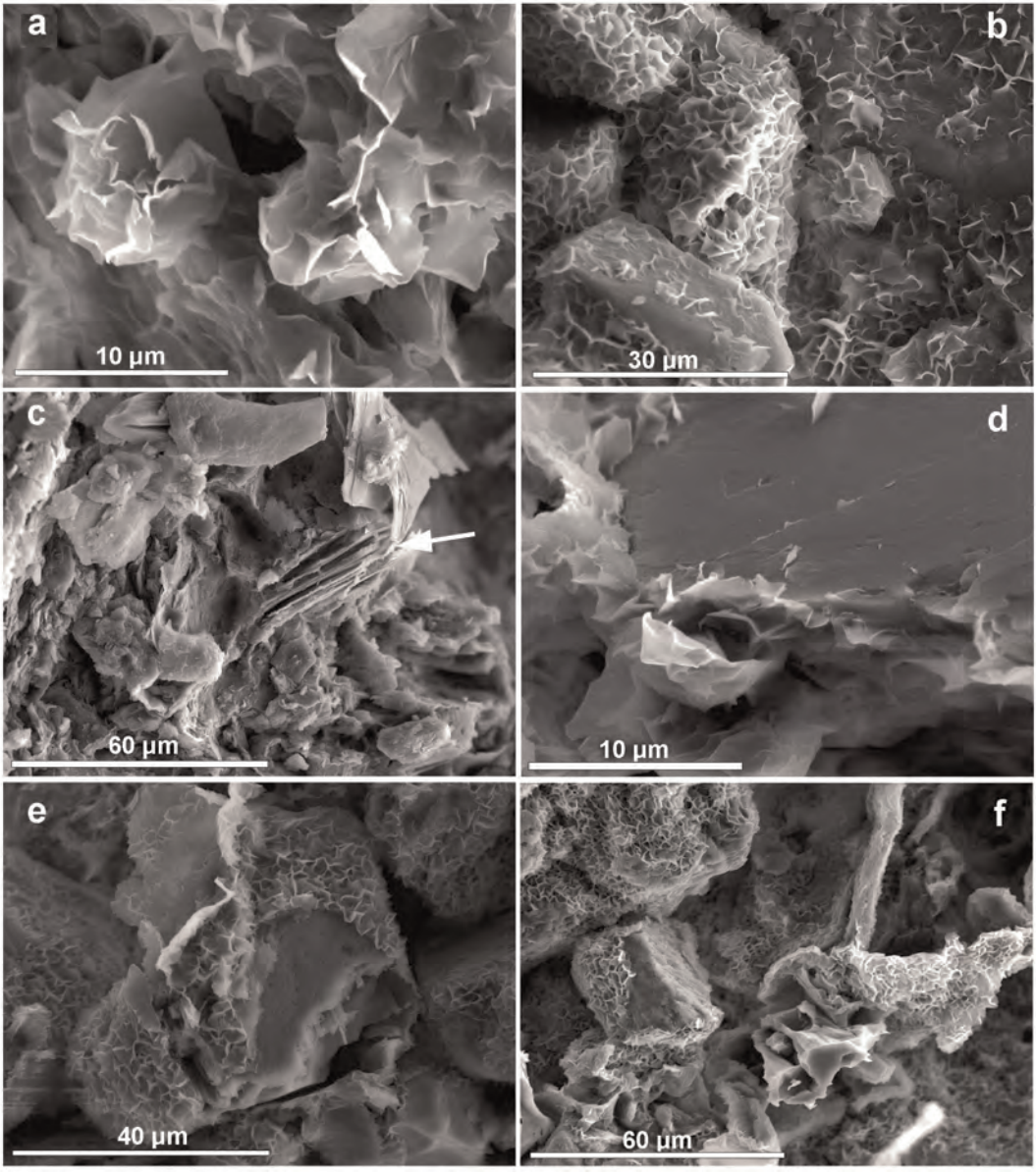

FIG. 3. SEM images of: (a) rose-shaped smectites; (b) small flakes of smectites covering detrital mineral surfaces; (c) general aspect of the micaceous sands samples. The arrow indicates the presence of sheets of open micas; (d) smectites growing on micas edges and fractures; (e) partial dissolution of feldspars and growth of smectites over them; and (f) general aspect of the arkosic samples, showing the development of smectite coatings on detrital grains.

Mineral chemistry

Micaceous and illitic compositions were obtained from EMPA study of coarse mica. Both dioctahedral and trioctahedral varieties are present. Trioctahedral micas correspond to biotite but they display large compositional variability (Table 2). The predominant interlayer cation is K and they display different layer charges as a result of

TABLE 2. Mean structural formulae of the Somosaguas micas, obtained by EMP analyses of isolated particles.

	Biotite				Muscovite			
	Mean n = 88	St. Dv.	Max	Min	Mean n = 15	St. Dv.	Max	Min
Si	5.95	0.25	6.81	5.50	6.44	0.36	7.15	6.14
^{IV}Al	2.05	0.25	2.50	1.19	1.56	0.36	1.86	0.85
^{VI}Al	1.12	0.25	1.68	0.60	3.45	0.23	3.70	3.01
Mg	1.50	0.28	2.06	0.66	0.24	0.15	0.60	0.11
Ti	0.35	0.08	0.48	0.01	0.05	0.05	0.11	0.02
Mn	0.03	0.01	0.08	0.00	0.03	0.02	0.06	0.00
Fe^{2+}	2.27	0.28	2.86	1.66	0.31	0.10	0.50	0.16
$\Sigma^{VI}R$	5.27	0.11	5.45	4.94	4.08	0.04	4.15	3.95
K	1.60	0.20	1.90	0.94	1.75	0.11	1.86	1.51
Ca	0.04	0.03	0.18	0.00	0.01	0.01	0.04	0.00
Na	0.02	1.01	0.08	0.00	0.11	0.07	0.19	0.00
C.L.	1.69	0.15	1.94	1.25	1.85	0.14	2.01	1.64

Number of cations on the basis of O_{20} $(OH)_2$. $\Sigma^{VI}R$: Number of octahedral positions occupied for a unit cell. C.L.: layer charge. St. Dv.: Standard deviation. Min: Minimum values. Max: Maximum values. n = number of samples.

different alteration degrees. In places small layer charges (1.94−1.25), typical of vermiculite, have been observed. All possible intermediate stages between mica and vermiculite layer charge can be observed. Biotite crystals display a continuous variation of Fe, Al and Mg content. Also, dioctahedral micas were found. They display considerable tetrahedral Al variation. The dioctahedral micas are muscovites, and also display important compositional variation. The tetrahedral Al varies from muscovite to near fengitic micas with low tetrahedral charge (layer charge from 1.86 to 0.85) (see Table 2).

The average structural formulae of smectites obtained by AEM correspond to dioctahedral smectites (Table 3). Both beidellitic and montmorollonitic end-members are present. Analysis number 1 corresponds to montmorillonite because of the dominant octahedral charge, whereas average formulae 2 to 4 correspond to beidellites with

TABLE 3. Mean structural formulae from the Somosaguas smectites samples, obtained by AEM.

	Montmorillonite		Beidellite		Fe-rich beidellite			
	Mean n = 7	St. Dv.	Mean n = 18	St. Dv.	Mean n = 10	St. Dv.	Mean n =10	St. Dv.
Si	7.82	0.07	6.90	0.35	7.13	0.36	6.46	0.44
^{IV}Al	0.18	0.07	1.10	0.35	0.87	0.36	1.54	0.44
^{VI}A	3.02	0.12	3.54	0.40	2.91	0.24	1.57	0.58
Mg	0.92	0.06	0.36	0.24	0.59	0.16	1.26	0.50
Ti	0.00	0.00	0.01	0.01	0.02	0.02	0.12	0.13
Fe^{3+}	0.20	0.12	0.39	0.14	0.75	0.11	1.64	0.30
$\Sigma^{VI}R$	4.14	0.04	4.29	0.10	4.28	0.15	4.59	0.21
K	0.03	0.01	0.27	0.31	0.17	0.14	0.74	0.36
Ca	0.33	0.02	0.13	0.07	0.24	0.11	0.10	0.06
Na	0.00	0.01	0.05	0.08	0.04	0.05	0.10	0.21
C.L.	0.68	0.05	0.55	0.25	0.63	0.19	0.91	0.24

Number of cations on the basis of O_{20} $(OH)_2$. $\Sigma^{VI}R$: Number of octahedral positions occupied for a unit cell. C.L.: layer charge for a unit cell. St. Dv.: Standard deviation. n = number of samples.

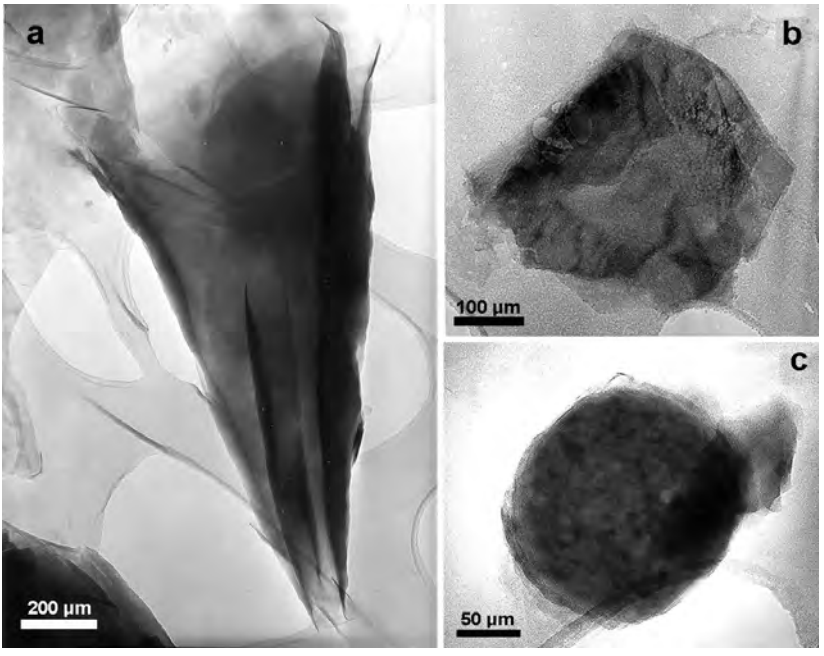

FIG. 4. TEM images showing typical smectite micromorphologies of the studied sediments. (a) Montmorillonite particles show thin curved layers with warped edges. (b) Beidellites show platy morphologies very similar to that of the micas. (c) Rounded beidellite particle.

dominant tetrahedral charge. Beidellites show great compositional variability (see standard deviation, Table 3), as a function of the Mg and Fe^{3+} content and the type of the predominant interlayer cation (K or Ca). Because of the large compositional variability, three groups of beidellite were differentiated on the basis of octahedral Fe contents. Compositional limits were established as follows (Brigatti & Poppi, 1981): (1) beidellites with <0.6 Fe^{3+} atoms per unit cell (average number 2, Table 3); (2) beidellites with $0.6 < Fe^{3+} < 1$ atoms per unit cell (average number 3, Table 3); and (3) beidellites with $Fe^{3+} > 1$ atoms per unit cell (average number 4, Table 3). Type 1 can be considered beidellites, and those of types 2 and 3 can be considered Fe-rich beidellites. The Mg contents and layer charge vary according to Fe content and opposite to Al content. Furthermore, some beidellites display a decrease in Fe and K and a slight enrichment in Ca toward the edges of the crystals. Ti is only found in beidellites.

DISCUSSION

The detrital materials studied have similar composition to the source materials, which were probably derived from the Spanish Central System (Guadarrama Range), as shown by the similar mineralogical composition of the micas (both dioctahedral and trioctahedral) of the Somosaguas detrital deposits and the Guadarrama granitic rocks (Aparicio *et al*., 1980; Huertas-Coronel, 1990; Villaseca & Barbero, 1994). The detrital materials show a close genetic relationship with the granitic and high-grade metamorphic rocks from Guadarrama Range, although occasional contribution of low-grade metamorphic rocks was found too. The inherited detrital micas have undergone important degradation processes. Also, slightly altered rock fragments of gneiss, quartzite, shale and phyllites, as well as small amounts of chlorites have been found, confirming the aforementioned source area materials.

The interpretation of XRD patterns, SEM, TEM, EMPA and optical microscopy data from the Somosaguas deposits reveals mineral mixtures of detrital (inherited), transformed and neoformed origin. In the area studied, clay minerals resulted from interactions between Guadarrama rocks (source area) and meteoric water. The most abundant minerals are phyllosilicates, followed by feldspars (Table 1). According to Pettijhon *et al*.

(1975), arkoses are typical products of granite alteration in semiarid regions, with sporadic torrential-type sediment transport. Rutile, tourmaline and apatite reflect the source area composition, since they are accessory minerals in the Guadarrama Range rocks.

The clastic minerals are quartz, feldspars, micas, kaolinite and chlorite. Some of these minerals have been altered, as a result of weathering and hydrolysis, either in the source area or during the transport, and in the sedimentary basin as well. In our samples the potassic feldspars (orthoclase and microcline) and plagioclases show signs of dissolution processes (Fig. 3e and f). These processes removal alkalis and alkaline earth elements for formation of kaolinite. According to Wilson (2004), plagioclases usually show a greater degradation degree than the potassic feldspars, due to their low stability in external conditions. In the studies carried out by Nixon (1979) feldspars underwent differential dissolution in energetically favourable zones, such as twin planes, crystallographic defects, fractures, etc. The alteration mechanism and the sequence of feldspars transformation into clays are controlled by dissolution-reprecipitation processes (Tsuzuki & Kawabe, 1983; Drief *et al*., 2001). The necessary conditions for transformation of feldspars into kaolinite occurred presumably in the source area (Spanish Central System), since kaolinite was transported to the basin.

Detailed study of micas by EMPA and TEM reveals that in most cases micas have been degraded resulting in illitic or even vermiculitic charges (Table 2), in accordance with Wilson (2004). This process may be followed by entrance of calcium in the interlayer space, finally yielding dioctahedral smectites (Table 3), and rarely kaolinite. In Fig. 5, interlayer potassium from all samples is projected against total iron content, and consequently two chemical trends can be distinguished. The first shows a transition from muscovites and dioctahedral illites to beidellites. The other trend is defined by the biotite degradation to beidellites with different layer charge and different octahedral Fe content. Figure 6 displays the relationship between octahedral occupancy and interlayer charge. Both dioctahedral and trioctahedral domains can be observed, as well as a continuous variation of the interlayer charge of the clay minerals. In the first alteration stage, interlayer potassium is partially lost, yielding illitic charge to the micas (Figs 5 and 6); ferrous Fe oxidizes to ferric Fe and an unbalanced charge is produced, similar to the experiments of Wilson (1975). The interlayer K of illitic charge micas is replaced by hydrated interlayer cations and a small rearrangement of the 2:1 structure is produced through dissolution-precipitation mechanism (Banfield & Eggleton, 1988; Drits *et al*., 1996; Drief & Nieto, 2000). Thus, the separation between the mica-type sheets increases and produces the break-up of their weak joints (Ahn & Peacor, 1986), which results in crystalline units getting progressively smaller as the exfoliation process advances. In the intermediate alteration stage, I-S mixed-layers are formed (Klimentidis, 1986; Veblen *et al*., 1990; Velde, 2001). This alteration sequence is of great interest because it reflects all the stages

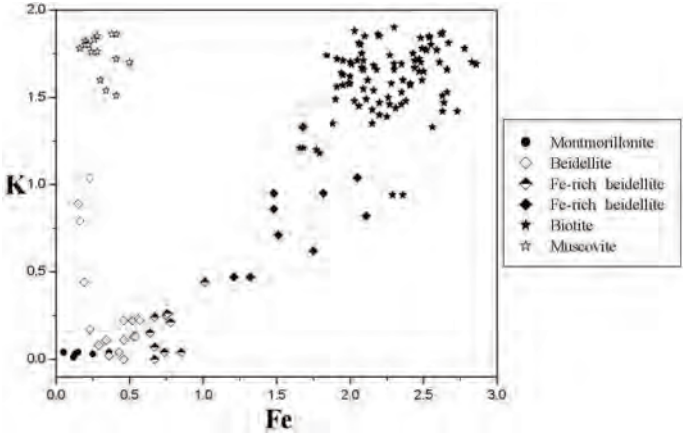

FIG. 5. Interlayer K *vs*. total Fe plot from clay minerals of the Somosaguas sediments.

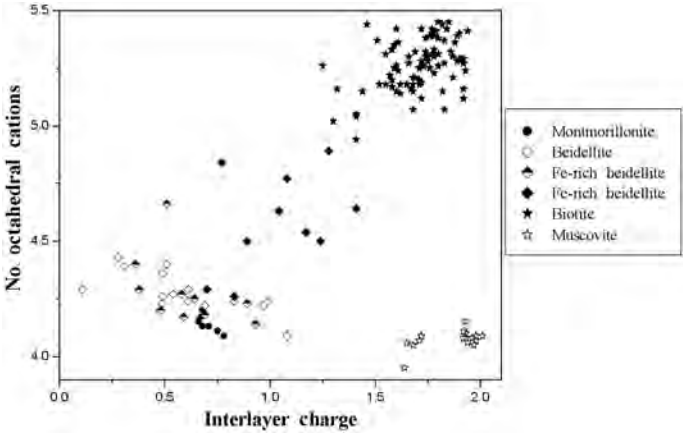

FIG. 6. Relationship between the number of octahedral cations and interlayer charge of the Somosaguas clay minerals.

of the degradation of these micas, and thus genetic processes. Moreover it supports the palaeoambiental data obtained up to now by palaeontological studies.

The most abundant neoformed phyllosilicates in the area studied are dioctahedral smectites, which indicate an Al-rich source. The observed smectites belong to two different groups, montmorillonites mainly with octahedral charge and beidellites mainly with tetrahedral charge (Table 3).

Montmorillonites have abundant octahedral Al and limited tetrahedral charge. Calcium is the major exchangeable cation, but limited interlayer K is also present (Table 3). Thin transparent flakes with warped edges are evident (Fig. 4a). The 'house of cards' and 'flake' habits of montmorillonites (Fig. 3b), along with the festooned edge morphologies distinguished by SEM (Fig. 3a), and the coating of detrital grains (Fig. 3e,f) may indicate that montmorillonites were formed *in situ*. Therefore, they would be interpreted as neoformed minerals, originating from hydrolysis and alteration of primary feldspar and muscovite in the ponds formed in distal zones of the alluvial fans.

Beidellite displays extensive compositional variation (Table 3), from Fe-Ti-rich to Fe-Ti-poor composition (Fig. 5). The most Fe-rich crystals, with Ti in octahedral positions, have different crystal forms (Figs 4b,c) and are genetically related to the trioctahedral micas of the source area. The less ferric phases may correspond to more advanced alteration stages of the same minerals or proceed from alteration of dioctahedral micas. Most of the Fe-rich beidellites have been described as products of alteration of micas: firstly micas with vermiculitic charge are formed, followed by Fe-rich beidellites preserving the tetrahedral charge (Badraoui *et al*., 1987; Badraoui & Bloom, 1990). Under TEM, the Fe-richest phases are generally rounded or with eroded edges (Fig. 4c). In many cases they have mica-type morphologies (Fig. 4b), which indicates transformation of one into the other. The Fe-poor crystals are semi-transparent and have more idiomorphic habits. Many of these particles show a compositional zonation, with an Fe-rich core and Fe-poor margins. This indicates an alteration sequence from less altered members richer in Fe, to more evolved Fe-poor ones. This process involves a certain charge loss, leading to the final formation of beidellites of lower interlayer charge (Figs 5 and 6).

Titanium is present only in beidellites, since it was present in the ferromagnesian minerals (mainly biotite) from which beidellite formed. This fact supports the idea that Fe-rich beidellites formed by the biotite degradation, whereas montmorillonites were formed *in situ*. The most abundant beidellites in the coarse size fraction (studied by EMPA) are those rich in Fe, whereas in the <2 μm fraction (AEM) they are Fe-poor.

The aforementioned observations describe a degradation process in which, initially, trioctahedral mica begins to alter and fracture, starting from the edges and the weakest zones of the crystal (Fig. 3c; Banfield & Eggleton, 1988). The K ions are replaced by hydrated ions (Drief & Nieto, 2000), and Fe^{2+}

transforms into Fe^{3+} (Gilkes *et al*., 1972), yielding micas of lower layer charge (Figs 5 and 6). While this process goes on, the total charge decreases (Fig. 6; Wilson, 1975), until Fe-rich beidellites are formed and small variations in the micaceous structure and the tetrahedral charge are produced (Gilkes *et al*., 1972). Subsequently, these particles break up into smaller crystals with greater specific surface area, so they alter more quickly and finally become Fe-impoverished beidellites. These processes, observed by electron microscopy, (Gilkes *et al*., 1972; Banfield & Eggleton, 1988; Drief & Nieto, 2000, among others) can be recognized in the SEM and TEM images obtained from the Somosaguas minerals and their respective chemical compositions. In the coarser fractions, inherited minerals predominate, whereas the concentration of transformed and neoformed minerals increases when the particle size diminishes.

The substantial compositional variations of beidellites, mainly Fe, but also Mg and Al (Table 3 and Figs 5 and 6) would indicate that some beidellites proceed from trioctahedral micas (biotite) and others from dioctahedral ones (muscovite) (Drief & Nieto, 2000), or may correspond to different mica alteration stages. The Fe-richest members are most abundant, and originate from biotite alteration. In Velde's diagram (Velde, 1985; Fig. 7), two alteration sequences are distinguished in the Somosaguas samples. On the one hand, a trend is observed between muscovites, dioctahedral illites and some of the beidellites. On the other hand, another trend is defined by the degradation of the biotite to Fe-rich beidellites, and finally to beidellites. The mixed-layer I-S is the intermediate step in the transformation process between micas and smectites (Velde, 2001).

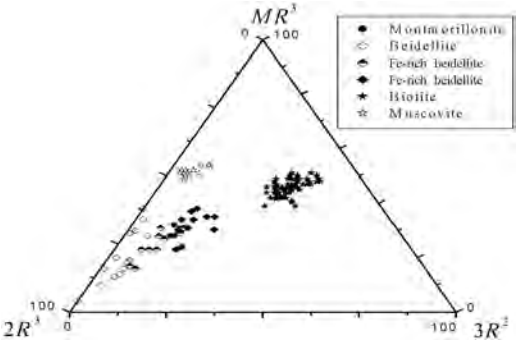

FIG. 7. Representation of AEM and EMPA data after Velde (1985). MR^3 = Na+K+2Ca; $2R^3$ = (Al+Fe^{3+})/2; $3R^2$ = (Mg+Fe^{2+})/3.

According to Paquet (1969), smectites are preferably formed in poorly drained soils with high pH or in zones with sufficient Mg supply, since this element favours the crystallization of smectites (Tomita; 1970; Harder, 1972; Wilson, 1999; Fiore *et al*., 2001). Basic cations and Si concentrate in poorly drained conditions, and yield montmorillonite neoformation irrespective of the climate (either tropical humid or dry) (Paquet, 1969; Tardy, 1969; Bocquier, 1971). Under sufficient drainage conditions, micas are altered to vermiculites and not to smectites, while in poorly drained conditions, beidellites form from biotites and mixed-layer I-S from muscovites (Aoudjit *et al*., 1995). The pH can also change, since in well drained zones (geomorphological highs) the pH is more acid (close to 5), while in poorly drained zones (geomorphological lows) the pH is neutral or slightly basic (close to 7), which favours montmorillonite formation. Thus, in well drained areas hydrolysis dominates and aluminium hydroxides precipitate, while K is washed out (Righi & Meunier, 1991). On the other hand, in poorly drained zones, montmorillonite neoformation results in the presence of Ca and Mg, while feldspars are dissolved and kaolinite forms (Aoudjit *et al*., 1995). Hence the formation of the smectites present in the Somosaguas sediments is indicative of relative poor drainage conditions.

CONCLUSIONS

The Al-rich clay minerals present in the Somosaguas Miocene sediments have formed from alteration of igneous and metamorphic rocks in the source area. No compositional correlation exists between them and the important deposits of magnesian clays in the central part of Madrid basin. Two mineralogical trends can be distinguished. One shows a clear evolution from muscovites to dioctahedral illites and beidellites. The other is defined by biotite, which was degraded to Fe-rich beidellites and finally to beidellites. Both trends are associated with an Fe and K loss, and simultaneously with layer-charge reduction. Mixed-layer I-S has been identified as the intermediate step in the transformation process between micas and smectites. This alteration sequence is of great interest because it reflects all the stages of degradation of micas and allows us to deduce genetic processes as well as to support the palaeoambiental data obtained so far by palaeontological studies.

ACKNOWLEDGMENTS

We thank Dr M. Suarez and Mr M.B. Said Fesharaki for helpful comments. We also express our sincere thanks to Catherine Doyle for checking and improving the English. Financial support was provided by UCM (Proyecto Somosaguas-910161) and CAM to the investigation group (number 910386). The constructive comments of Drs N. Güven, G. Christidis and an anonymous referee improved the text.

REFERENCES

Ahn J.H. & Peacor D.R. (1986) Transmission and analytical electron microscopy of the smectite to illite transmission. *Clays and Clay Minerals*, **34**, 165–179.

Alonso-Zarza A.M. & Fort R. (1991) Caracterización mineralógica de las arenas miocenas del margen NE de la Cuenca de Madrid: aplicación a los estudios de procedencia. *Estudios Geológicos*, **47**, 157–168.

Alonso-Zarza A.M., Calvo J.P. & García Del Cura M.A. (1992) Palustrine sedimentation and associated features (grainification and pseudo-microkarst) in the Middle Miocene (Intermediate Unit) of the Madrid basin, Spain. *Sedimentary Geology*, **76**, 43–61.

Alonso-Zarza A.M., Calvo J.P., García Del Cura M.A. & Hoyos M. (1990) Los sistemas aluviales miocenos del borde Noreste de la Cuenca de Madrid: sector Cifuentes-Las Inviernas (Guadalajara). *Revista Sociedad Geológica de España*, **3**, 1–2.

Alonso-Zarza A.M., Calvo J.P., Silva P.G. & Torres T. (2004) Cuenca del Tajo. Pp. 556–560 in: *Geología de España* (J.A. Vera, editor). IGME, Madrid.

Aoudjit H., Robert M., Elsass F. & Curmi P. (1995) Detailed study of smectite genesis in granitic saprolites by analytical electron microscopy. *Clay Minerals*, **30**, 135–147.

Aparicio A., Bellido F., García Cacho L. & López Ruiz J. (1980) Evolución química de las biotitas y moscovitas de las rocas graníticas de las sierras de Guadarrama y Gredos (Sistema Central), durante los procesos de diferenciación magmática. *Estudios Geológicos*, **36**, 307–317.

Badraoui M. & Bloom P.R. (1990) Iron rich high charge beidellite in vertisols and mollisols of the high Chaouia Region of Morocco. *Soil Science Society of America Journal*, **54**, 267–274.

Badraoui M., Bloom P.R. & Rust R.H. (1987) Occurrence of high charge beidellite in vertic haplacuoll of Northwestern Minnesota. *Soil Science Society of America Journal*, **51**, 813–818.

Banfield J.F. & Eggleton R.A. (1988) A transmission electron microscope study of biotite weathering. *Clays and Clay Minerals*, **36**, 47–60.

Benayas J., Pérez Mateos J. & Riba O. (1960) Asociaciones de minerales detríticos en los sedimentos de la cuenca del Tajo. *Anales de Edafología y Agrobiología*, **11**, 633–670.

Bocquieur G. (1971) *Genèse et évolution de deux toposéquences de sols tropicaux du Tchad. Interprétation biogéodynamique*. Thèse de Docteur es Sciences de la Faculté de Science de l'Université de Strasbourg, France.

Brigatti M.F. & Poppi L. (1981) A mathematical model to distinguish the members of the dioctahedral smectite series. *Clay Minerals*, **16**, 81–89.

Bustillo M.A. (1976) Estudio petrológico de las rocas silíceas miocenas de la Cuenca del Tajo. *Estudios Geológicos*, **32**, 451–497.

Bustillo M.A. & Bustillo M. (1988) Características diferenciales e interpretación genética de ópalos constituidos en sedimentos biosilíceos y ópalos inorgánicos (Esquivias, Cuenca de Madrid). *Boletín Geológico y Minero*, **99**, 615–627.

Bustillo M.A. & Capitán J. (1990) Secuencias ópalo-arcillosas en zona de borde de lago (Vicálvaro, Cuenca del Tajo). *Boletín Geológico y Minero*, **101**, 932–944.

Calvo J.P., Ordóñez S., Hoyos M. & García Del Cura M.A. (1984) Caracterización sedimentológica de la Unidad Intermedia del Mioceno de la zona Sur de Madrid. *Revista Materiales y Procesos Geológicos*, **2**, 145–176.

Calvo J.P., Alonso Zarza A.M. & Garcia del Cura M.A. (1989) Models of Miocene marginal lacustrine sedimentation in response to varied depositional regimes and source areas in the Madrid Basin (Central Spain). *Palaeogeography, Palaeoclimatology, Palaeoecology*, **70**, 199–214.

De Vicente G., Calvo J.P. & Muñoz A. (1996a) Neogene tectono-sedimentary review of the Madrid Basin. Pp. 268–271 in: *Tertiary Basins of Spain* (P.F. Friend & C.J. Dabrio, editors). Cambridge University Press, UK.

De Vicente G., González-Casado J.M., Muñoz-Martín A., Giner J.L. & Rodríguez Pascua M.A. (1996b) Structure and Tertiary evolution of the Madrid Basin. Pp. 263–267 in: *Tertiary Basins of Spain* (P.F. Friend & C.J. Dabrio, editors). Cambridge University Press, UK.

Domínguez Díaz M.C. (1994) *Mineralogía y sedimentología del Neógeno del sector centro occidental de la Cuenca del Tajo*. Tesis Doctoral. Facultad de Ciencias Geológicas. Universidad Complutense de Madrid, Spain, 309 pp.

Domínguez Díaz M.C., Doval M., García Romero E. & Brell J.M. (1996) Análisis de los procesos de formación de minerales de la unidad de arcosas de la cuenca del Tajo. *Geogaceta*, **20**, 1488–1491.

Drief A. & Nieto F. (2000) Chemical composition of smectites formed in clastic sediments. Implications

for smectite-illite transformation. *Clay Minerals*, **35**, 665–678.

Drief A., Nieto F. & Sanchez-Navas S. (2001) Experimental clay-mineral formation from a sub-volcanic rock by interaction with 1 M NaOH solution at room temperature. *Clays and Clay Minerals*, **49**, 92–106.

Drits V.A., Salyn A.L. & Šuchá V. (1996) Structural transformations of interstratified illite-smectite from Dolna Ves hydrothermal deposits: Dynamics and mechanisms. *Clays and Clay Minerals*, **44**, 181–190.

Fiore S., Huertas F.J., Huertas F. & Linares J. (2001) Smectite formation in rhyolitic obsidian as inferred by microscopic (SEM-TEM-AEM) investigation. *Clay Minerals*, **36**, 489–500.

Gilkes R.J., Young R.C. & Quirk J.P. (1972) The oxidation of octahedral iron in biotite. *Clays and Clay Minerals*, **20**, 303–315.

Harder H. (1972) The role of magnesium in the formation of smectite minerals. *Chemical Geology*, **10**, 31–39.

Huertas-Coronel M.J. (1990) *Las asociaciones filonianas tardihercínicas de la sierra de Guadarrama (Sistema Central español)*. Tesis Doctoral. Facultad de Ciencias Geológicas, Universidad Complutense de Madrid, España, 335 pp.

Jackson M.L. (1975) *Soil Chemical Analysis. Advanced Course*. University of Wisconsin, College of Agriculture, Department of Soils, Madison, Wisconsin, USA.

Jarosewich E., Nelen J.A. & Norberg A. (1980) Reference samples for electron microprobe analysis. *Geostandards Newsletter*, **4**, 43–47.

Klimentidis R.E. (1986) High resolution imaging of ordered mixed-layer clays. *Clays and Clay Minerals*, **34**, 155–164.

Lomoschitz A., Calvo J.P. & Ordoñez S. (1985) Sedimentología de las facies detríticas de la Unidad Intermedia del Mioceno al Sur y Este de Madrid. *Estudios Geológicos*, **41**, 343–358.

López-Martínez N., Élez J., Hernando J.M., Luis A., Mazo A., Mínguez Gandú D., Morales J., Polonio I., Salesa M.J. & Sánchez I. (2000a) Los vertebrados fósiles de Somosaguas (Pozuelo, Madrid). *Coloquios de Paleontología*, **51**, 69–86.

López-Martínez N., Élez J., Hernando J.M., Luis A., Mínguez D., Polonio I., Salesa M.J., Mazo A. & Sánchez I. (2000b) Los vertebrados fósiles de Somosaguas (Pozuelo de Alarcón, Madrid). Pp. 130–140 in: *Patrimonio paleontológico de la Comunidad de Madrid* (J. Morales *et al*., editors). Consejería de Educación de la Comunidad de Madrid, España.

Luis A. & Hernando J.M., (2000) Los microvertebrados fósiles del Mioceno Medio de Somosagus Sur (Pozuelo de Alarcón, Madrid, España). *Coloquios de Paleontología*, **51**, 87–136.

Megías A.G., Leguey S. & Ordoñez S. (1982) Interpretación tectosedimentaria de la génesis de fibrosos de la arcilla en series detríticas continentales. (Cuencas de Madrid y del Duero, España). *Quinto Congreso Latino-Americano de geología*. Buenos Aires, Argentina.

Mínguez Gandú D. (2000) Marco estratigráfico y sedimentológico de los yacimientos paleontológicos miocenos de Somosaguas (Madrid, España). *Coloquios de Paleontología*, **51**, 183–196.

Moore D.M. & Reynolds R.C. (1989) *X-ray Diffraction and the Identification and Analysis of Clay Minerals*. Oxford University Press, New York.

Nixon R.A. (1979) Differences in incongruent weathering of plagioclase and microcline cation leaching versus precipitates. *Geology*, **7**, 221–224.

Ordoñez S., Fontes Ch. & García del Cura M.A. (1983) Contribución al conocimiento de la sedimentogénesis evaporítica de las cuencas neógenas de Madrid y del Duero en base a los datos de isótopos estables ($\delta^{13}C$, $\delta^{18}O$, $\delta^{34}S$). *X Congreso Nacional de Sedimentología, Menorca, Spain*, 49–52.

Paquet H. (1969) *Evolution géochimique des minéraux argileux dans les altérations et les sols des climats méditerranées et tropicaux á saisons contrastées*. Thèse de Docteur es Sciences de la Faculté de Science de l'Université de Strasbourg, France.

Pettijohn F.J. (1975) *Sedimentary Rocks*. Harper and Row, New York, 628 pp.

Polonio I. & López-Martínez N. (2000) Análisis tafonómico de los yacimientos de Somosaguas (Mioceno Medio, Madrid). *Coloquios de Paleontología*, **51**, 235–266.

Regueiro M., Lombardero M. & Gonzalo Corral F. (2002) Áridos, piedra natural y minerales industriales. *XI International Mining and Metallurgy Congress, Zaragoza (Spain).*

Riba O. (1959) Ensayo sobre la distribución de litofacies del Terciario continental de la Cuenca del Tajo al W de la Sierra de Altomira. *Cursillos y Conferencias. Instituto Lucas Mallada*, **4**, 171.

Righi D. & Meunier A. (1991) Characterization and genetic interpretation of clays in acid brown soil (Dystrochrept) developed in a granitic saprolite. *Clays and Clay Minerals*, **39**, 519–530.

Rodríguez Aranda J.P., Calvo J.P. & Ordoñez S. (1991) Transición de abanicos aluviales a evaporitas en el Mioceno del borde oriental de la cuenca de Madrid (sector Barajas de Melo-Illana). *Revista de la Sociedad Geológica de España*, **4**, 33–50.

Schultz L.G. (1964) Quantitative interpretation of mineralogical composition from X-ray and chemical data for the Pierre Shale. *US Geological Survey Bulletin Professional Paper* **391-c**, 31 pp.

Tardy Y. (1969) *Géochimie des altérations; étude des arénes et des eaux de quelques massifs cristallins*

d'Europe et d'Afrique. Thèse de Docteur es Sciences de la Faculté de Science de l'Université de Strasbourg, France.

Tomita K. (1970) Syntheses montmorillonite and vermiculite-like minerals from sericite and pyrophyllite. *Journal of the Japanese Association of Mineralogists, Petrologists and Economic Geologists*, **63**, 109–121.

Tsuzuki Y. & Kawabe I. (1983) Polymorphic transformations of kaolin minerals in aqueous solutions. *Geochimica et Cosmochimica Acta*, **47**, 59–66.

Veblen D.R., Gutrie G.D., Livi K.J.T. & Reynolds R.C. Jr. (1990) High resolution transmission electron microscopy and electron diffraction of mixed-layer illite/smectite. Experimental results. *Clays and Clay Minerals*, **38**, 1–13.

Vegas R. & Banda S. (1982) Tectonic framework and Alpine evolution of the Iberian Peninsula. *Earth Evolution Sciences*, **4**, 320–343.

Velde B. (1985) *Clay Minerals. A Physico-chemical Explanation of their Occurrence*. Developments in Sedimentology, **40**, Elsevier, Amsterdam, 218 pp.

Velde B. (2001) Clay minerals in the agricultural surface soils in the Central United States. *Clay Minerals*, **36**, 277–294.

Villaseca C., Andonaegui P. & Barbero L. (1993) *Mapa geológico del plutonismo Hercínico de la región central española (Sierra de Guadarrama y Montes de Toledo) (1:150.000)*. Servicio Publicaciones CSIC, Madrid.

Villaseca C. & Barbero L. (1994) Chemical variability of Al-Ti-Fe-Mg minerals in peraluminous granitoid rocks from central Spain. *European Journal of Mineralogy*, **6**, 691–710.

Wilson M.J. (1975) Chemical weathering of some rock-forming minerals. *Soil Science*, **119**, 345–349.

Wilson M.J. (1999) The origin and formation of clay minerals in soils: past, present and future perspectives. *Clay Minerals*, **34**, 7–25.

Wilson M.J. (2004) Weathering of the primary rock-forming minerals: processes, products and rates. *Clay Minerals*, **39**, 233–266.